Resolving the Landauer paradox in ferroelectric switching by high-field charge injection

An-Quan Jiang,[1,*] Hyun Ju Lee,[2] Cheol Seong Hwang,[2,†] and Ting-Ao Tang[1]
[1]*ASIC & System State Key Laboratory, Department of Microelectronics, Fudan University, Shanghai 200433, China*
[2]*Department of Materials Science and Engineering and Inter-university Semiconductor Research Center, Seoul National University, Seoul 151-744, Korea*

(Received 2 January 2009; revised manuscript received 8 June 2009; published 31 July 2009)

The critical dimension for reverse domain nucleation in the ferroelectric polarization switching of $Pb(Zr_{0.4}Ti_{0.6})O_3$ (PZT) thin film was estimated experimentally from a coercive voltage estimation in $Pt/Al_2O_3/PZT/Ir$ ferroelectric thin-film capacitors with various Al_2O_3 thicknesses and switching currents. The critical nuclei dimension for reverse domain formation in a 300-nm-thick PZT was only 4.5 ± 0.4 nm, which is in agreement with theoretical predictions of the critical nucleus size. Almost all the coercive voltage was applied to the nucleation layer thickness during ferroelectric switching. The classical Merz's exponential law for the domain velocity description and Laudauer's paradox of an implausibly large nucleation energy barrier were understood in terms of the charge-injection limited domain motion described by thermionic field emission at the Pt/Al_2O_3 interface or Fowler-Nordheim tunneling at the Pt/PZT interface.

DOI: 10.1103/PhysRevB.80.024119 PACS number(s): 77.80.Fm, 73.40.Rw, 77.55.+f

I. INTRODUCTION

Polarization reversal in ferroelectric thin films under a reverse electric field is generally understood by the nucleation of oppositely polarized domains, preferably on surfaces or at defect aggregates in the films, and its propagation throughout the film thickness.[1–8] Experimentally, nuclei form thermally with an activation energy on the order of a few tens of k_BT,[3,4] where T is temperature and k_B is the Boltzmann constant. The activation energy consists mainly of the depolarization energy, W_d, due to the divergence of the spontaneous polarization on the edge of the reversed nucleus (domain) wall, and the domain-wall energy W_s. According to Landauer's calculations, the two values are $\sim 10^8 k_BT$ and $10^6 k_BT$, respectively, which are far larger than the experimentally determined value.[5] This is called Landauer's paradox. When the W_d was neglected by, for example, free-charge compensation, Merz derived an exponential law of domain velocity (ν) as a function of the electric field (E) with $\nu \propto \exp(-\delta/E)$,[9] where δ is the thermal activation field. However, most oxide ferroelectrics are highly insulating, and the process of free-charge compensation must be extremely slow compared with the high speed of domain penetration. Therefore, Molotskii *et al.* suggested the possibility of rapid charge compensation through electron tunneling from the electrode into the region where spontaneous polarization fluctuates.[10] This conception can resolve the Landauer's paradox; i.e., when the depolarization field (E_d) is high enough, carriers can be injected into the domain wall through a fast transport mechanism, which largely reduces the W_d and makes nucleation possible. As polarization reversal is a nucleation and growth process, there must be a critical nuclei dimension over which the stable nuclei present and subsequently grow. Although this critical dimension has been estimated theoretically by molecular-dynamics simulations,[7] no clear experimental evidence for this dimension and the charge injection has been reported. It is expected that direct observation of this critical nuclei dimension by any microscopic method is extremely difficult on account of its nm-scale dimension and fast moving speed.

One promising way of experimentally estimating this dimension is to estimate the amount of switching charge (Q_{sw}) necessary to initiate reverse domain nucleation. This assumes that Q_{sw} corresponds to the charge necessary to mitigate W_d during nucleation of the critical reverse domain. The switching current (I_{sw}, where $Q_{sw} = \int I_{sw} dt$, t is switching time) can be controlled by varying the load resistance (R_l) connected to the ferroelectric capacitor and the coercive voltage (V_c) of the ferroelectric capacitor is also controlled by the R_l. The threshold field for the charge injection (E_{th}) can be acquired from the V_c, and the E_{th} can be used to extract the critical dimension for reverse domain nucleation. This is from the relationship of $E_{th} = V_{fc}/d_f$, where V_{fc} is the coercive voltage of the reverse domain with the critical dimension of d_f. In addition, the relationship between I_{sw} and E_{th} can be used to confirm whether the acquired parameters are reasonable. There is one more independent parameter that can control V_c, which offers another dimension for achieving E_{th}. It was recently reported that an ultrathin dielectric layer (Al_2O_3) interposed between the ferroelectric $Pb(Zr,Ti)O_3$ (PZT) layer and Pt electrode works as a tunnel switch that opens up during ferroelectric switching.[11] Therefore, the V_c of the Al_2O_3/PZT stacked layer can be controlled for a given R_l with different thicknesses of the interposed Al_2O_3 layer. Therefore, the appropriate combination of R_l and Al_2O_3 layer thickness offers a unique opportunity to examine experimentally the critical dimension of ferroelectric domain reversal and the switching kinetics.

II. EXPERIMENTAL PROCEDURE; THE SAMPLE PREPARATION, STRUCTURAL CHARACTERIZATIONS, AND ELECTRICAL MEASUREMENTS

Details of sample fabrication, including the metal-organic chemical-vapor deposition (MOCVD) of PZT thin films, atomic layer deposition (ALD) of Al_2O_3 layer on top of the PZT, are reported in the on-line supporting information of Ref. 11. $Pt/Al_2O_3/PZT/Ir$ stacked ferroelectric capacitors were fabricated with varying Al_2O_3 layer thicknesses (d_{Al}

=1–6 nm, grown by ALD at 250 °C) deposited on a 300-nm-thick PZT (Zr:Ti=4:6) film grown by MOCVD at 620 °C on an Ir bottom electrode. The PZT films have a (111)-preferred growth behavior and deposition of the Al_2O_3 layer does not influence the structure or chemical properties of the PZT films. The structural characterization results are also included in the on-line supporting information of Ref. 11. For the electrical measurements, 80-nm-thick (111) Pt electrodes, with an area of $\sim 6.1\times10^{-4}$ cm^2, were deposited by electron-beam evaporation at room temperature using a metal shadow mask. The accurate area of each measured capacitor was determined by optical microscopy. The polarization-voltage (*P-V*) loops were checked using the Aixacct TF-2000 ferroelectric analyzer and a Radiant Precision Materials analyzer with a triangular wave form at a frequency of 1 kHz in the virtual ground mode. The ferroelectric switching kinetics and parameters were investigated using the pulsed domain switching experiment. Before the measurements, all the films were prepolarized negatively on the top electrodes and left for 2–3 months to reduce the imprint uncertainty of prepolarization history on the measurements in different films as much as possible. After each measurement, the final polarization was always returned into this direction. Two sequential square pulses with opposite polarities for domain switching measurements were supplied by an Agilent 81150A arbitrary wave form generator with a maximum voltage of 20 V and an internal resistance of 50 Ω. The domain switching current I_{sw} across the total loading resistor in the circuit was monitored using an oscilloscope (LC WR 6200A) with an internal resistance of either 50 Ω or 1 MΩ. Voltage (V_l) across R_l was calculated from this measurement. Each measurement was averaged three times, and each datum had high reproducibility during the measurements.

For the V_c determination from the *P-V* hysteresis loops at different temperatures the I_{sw} was determined mainly by the measurement frequency. Compared to the pulse measurements, the estimation of the I_{sw} is not an easy task from the *P-V* loops directly. Therefore, the shortcoming of this characterization should be obvious. However, as the temperature was decreased, the V_c became larger than the maximum voltage (20 V) of the pulse generator. Due to this difficulty, it was not possible to use the pulse-switching tests to calculate the V_c with different R_l at low temperatures.

III. RESULTS AND DISCUSSIONS

Quantum mechanical electron/hole tunneling can occur with a high probability in very thin films with a thin Schottky barrier below a few nanometers or in thicker films under an extremely high field. An extremely high electric field is necessary [$\sim$15 MV/cm for (001) $PbTiO_3$ as $\sim P_s/\varepsilon_0\varepsilon_f$, with $P_s=0.76$ Cm^{-2} and $\varepsilon_f=60$, where ε_f is the dielectric constant along the ⟨001⟩ direction of $PbTiO_3$] if charge injection is essential for the stable nucleation of the reverse domain. This suggests that E_d is applied over a very small thickness of d_f (in order of only a few nm).

In the early stages of ferroelectric switching in thin films, the domain grows by nucleation with a critical size. Once the nucleus reaches a critical length (l_{cr}) in the direction perpendicular to the film surface, the domain can penetrate into the film thickness, where the field is practically zero.[12] The driving force in the latter stage of domain penetration is the dissipation of depolarization energy to compensate for the formation of a newly formed domain wall. The theoretically estimated l_{cr} value in $PbTiO_3$ at 220 K under an electric field of 0.5 MV/cm is 5.3 and 1.2 nm for triangular and square shaped reverse domains, respectively.[7] The voltage dropped over the ferroelectric layer is maintained at V_c during polarization switching.[11,13] In addition, V_c is mostly dropped across the critical nuclei at the beginning of domain nucleation. When a voltage, V_a, is applied, $V_a=V_c+V_t$, where V_t is the voltage drop over all the parasitic in-series resistance R_t. R_t consists of the contact resistance between the electrode and dielecric film, and the total loading resistance R_l. R_l consists of the externally inserted resistance and the internal resistances of the voltage source and the oscilloscope for the pulse-switching set-up.[11,13] Therefore, the voltage across R_l during domain switching is as follows:

$$V_l = \frac{R_l}{R_t}(V_a - V_c), \tag{1}$$

with the relationship of $I_{sw}=V_l/R_l=(V_a-V_c)/R_t$. This type of domain switching is a current limited process with $v\propto I_{sw}$. v can be smaller in magnitude by more than five decades if R_l is increased from 100 Ω to 11 MΩ. With Eq. (1), V_c can be determined accurately from the measurement of V_l as a function of V_a for a given Al_2O_3 thickness and R_l. Actually, the switching current $I_{sw}=V_l/R_l$ also changes with V_a so that V_c is no longer a constant. However, if the change in V_a is small, such as 1–2 times in this measurement, the V_c variation is small enough for the above assumption to be valid.

The Al_2O_3 layer is a typical insulator under low fields but conducts current fluently under high fields through either Schottky emission or thermionic field emission.[11] This is because during polarization switching, a huge field is applied to the dielectric Al_2O_3 layer and the domains within the Al_2O_3/PZT bilayers can be switched but with a higher apparent V_c due to the voltage drop across this layer.[11]

Figure 1(a) shows the typical pulse-switching behavior, where the voltage transients (V_l) over the R_l (from 100 Ω to 11 MΩ) with time are shown when $d_{Al}=6.0$ nm. Details for the pulse-switching measurement are reported elsewhere.[11,13] Transient I_{sw} as a function of time can be achieved by dividing V_l with R_l. After initial capacitor charging (peak near $t=0$), V_l (or I_{sw}) shows a plateau up to a certain time (polarization switching time). The area under each I_{sw} curve at a given R_l excluding the pure capacitor charging component corresponds to Q_{sw}, which must be independent of R_l. The plateau height is proportional to V_a, as shown in Fig. 1(b). V_c at different R_l was derived from a linear fit of the plateau heights to Eq. (1). V_c increases rapidly with decreasing R_l due to the increasing voltage sharing of the ferroelectric capacitor with decreasing R_l. However, it should be noted that V_c is nonlinearly dependent on I_{sw}. V_c at different R_l and d_{Al} was achieved from a fit of the data shown in Fig. 1(b) to Eq. (1). The results are plotted as a function of d_{Al} for a given R_l [Fig. 2(a)].

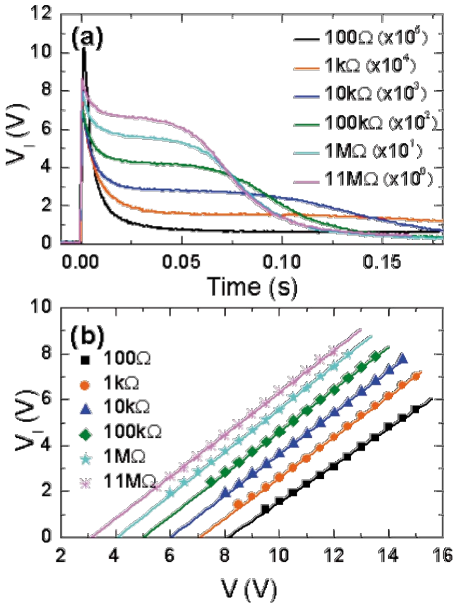

FIG. 1. (Color online) (a) Voltage transient across different R_l during domain switching under $V=13.0$ V for an Al_2O_3/PZT bilayer with $d_{Al}=6.0$ nm. The time scale was magnified by a factor shown in the parenthesis in the legend so that all wave forms at different R_l can be plotted together. (b) Voltage dependence of the step height across different R_l for an Al_2O_3/PZT bilayer with $d_{Al}=2.0$ nm. The solid lines are the best fit of the data to Eq. (1).

The V_c of the Al_2O_3/PZT bilayer consists of a coercive voltage V_{fc} for the domain switching of PZT and the threshold voltage V_{th} for the Al_2O_3 layer for it to be sufficiently conducting.[11] Therefore, $V_c=V_{fc}+V_{th}$. With $V_{th}=d_{Al}E_{th}$, E_{th} across the Al_2O_3 is acquired from Eq. (2) as follows:

$$E_{th}=\left.\frac{dV_c}{dd_{Al}}\right|_{I_{sw}=\text{const}}. \quad (2)$$

As Fig. 2(a) shows a linear dependency of V_c on d_{Al} when $d_{Al}>0$ nm, E_{th} can be calculated at each R_l. Apparently, there is a large deviation of the data from the linear fits at $d_{Al}=0$, suggesting that the threshold field for the Pt/PZT interface is different from that for the Pt/Al_2O_3 interface. The most important finding from the linear fits is that the line of best fits intercepts the x axis exactly at the same point (d_f^{Al}) with $d_f^{Al}=-2.2\pm0.2$ nm. This $|d_f^{Al}|$ value is believed to correspond to the Al_2O_3 equivalent critical nuclei dimension of the reversed domain of PZT under a switching field. This can be explained by the following: when $V_c=0$, $V_{fc}=-d_f^{Al}E_{th}$. Since there is no Al_2O_3 layer when $d_{Al}<0$, the term $d_f^{Al}E_{th}$ should be replaced with $d_fE'_{th}$, where E'_{th} is the threshold field for charge injection for the Pt/PZT interface. Since the critical amount of charge injection, Q_{sw}, necessary to induce the formation of stable nuclei should be irrespective of the presence of an Al_2O_3 layer, $C_{Al}V_{Al}=C_{PZT}V_{PZT}$ (or $\varepsilon_{Al}E_{th}=\varepsilon_{PZT}E'_{th}$, where ε_{Al} and ε_{PZT} are the optical dielectric constants of Al_2O_3 and PZT layers, respectively.), where C_{Al} and V_{Al} are the capacitance of the Al_2O_3 layer and voltage applied to the Al_2O_3 layer during switching, respectively. C_{PZT} and V_{PZT} have the same meaning as the polarization reversed

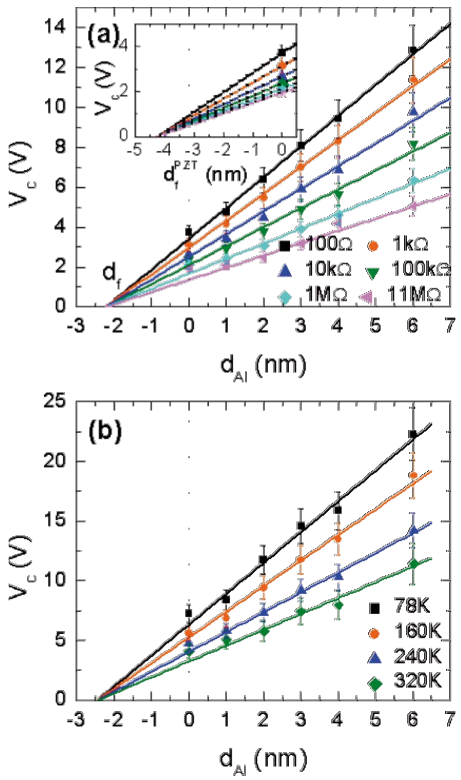

FIG. 2. (Color online) (a) d_{Al} dependence of V_c for the Al_2O_3/PZT bilayer with different R_l. V_c was derived from pulse measurements at $T=290$ K. (b) d_{Al} dependence of V_c for the Al_2O_3/PZT bilayer at different temperatures, where V_c was derived from the P-V hysteresis loop at 1 kHz.

PZT region with the dimension of d_f. Since the carriers are moving rapidly through either the Al_2O_3 or PZT layer, the optical dielectric constant must be the proper dielectric constant that determines the capacitance,[14,15] which are 2.9 and 5.6 for the Al_2O_3 and PZT thin films, respectively. Therefore, $E'_{th}=0.52E_{th}$, and $d_f=1.93d_F^{Al}$. This suggests that the critical dimension for a reversely polarized domain is 4.2 ± 0.4 nm. The critical dimension is along the depth direction of the PZT film estimated from the electrode/PZT (or Al_2O_3/PZT) interface.

Switching-charge-injection-dominated polarization reversal can also be checked by measuring the P-V hysteresis loops at different temperatures under a given R_l value but with a different d_{Al}, because charge injection can be controlled thermally. This is the third variable that can be used to determine d_f. For the V_c determination from the P-V hysteresis loops at different temperatures, as shown in Figs. 3(a) and 3(b) for $d_{Al}=3.0$ and 6.0 nm, respectively, the I_{sw} is determined mainly by the measurement frequency. Since the same frequency was used for all measurements at different temperatures, the I_{sw} was almost identical in all the extractions of V_c from the V_a-V_l plots at various temperatures, even though a slight difference in the applied voltage can cause a slight change in I_{sw}.

Figure 2(b) shows the change in V_c as a function of d_{Al} at different temperatures obtained from the P-V loop measurements shown in Fig. 3. All the data except for those at $d_{Al}=0$ show a linear dependence, and all linear fits intercept the

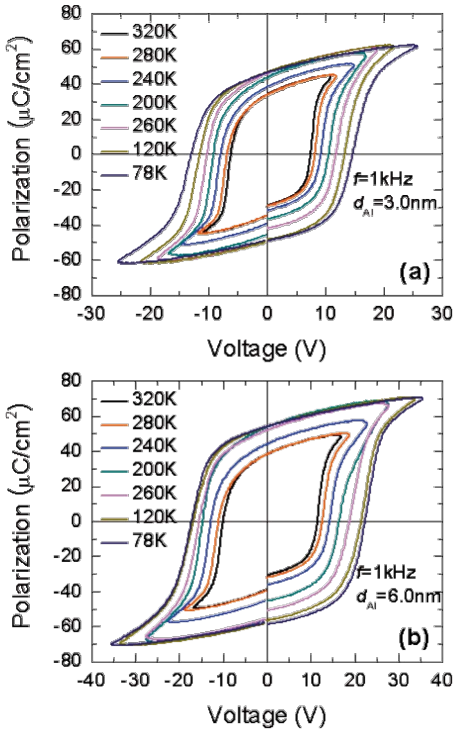

FIG. 3. (Color online) *P-V* hysteresis loops at different temperatures for (a) $d_{\mathrm{Al}}=3.0$ nm and (b) 6.0 nm,

x axis at $d_{\mathrm{f}}^{\mathrm{Al}}=-2.5\pm0.3$ nm ($d_{\mathrm{f}}=4.8\pm0.4$ nm) at temperatures ranging from 78 to 320 K. This $|d_{\mathrm{f}}^{\mathrm{Al}}|$ is slightly higher than that determined from previous measurements but still within the limits of experimental error. These results clearly show that the critical nuclei dimension for a PZT film is 4.2–4.8 nm, which is in very good agreement with the theoretical calculation results.[7]

As I_{sw} is controlled by the R_l, E_{th} is also dependent on the R_l. Therefore, there must be a physical relationship between I_{sw} and E_{th}. Figure 4(a) shows the change in switching current density (J_{sw}), which was taken at $V_l=4.0$ V at each R_l

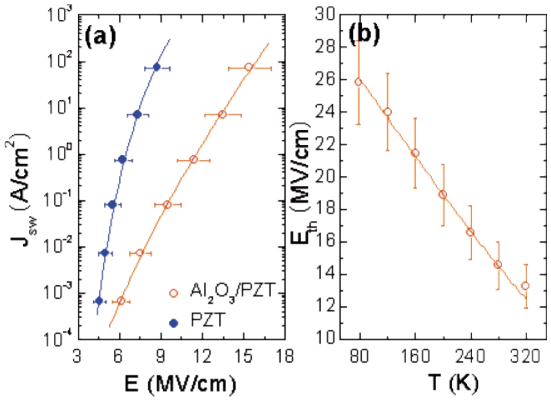

FIG. 4. (Color online) (a) Field dependence of the switching current density at $T=290$ K across the constituents, PZT and Al_2O_3, in the Al_2O_3/PZT bilayer with the data fitted by the solid lines to Eqs. (5) and (3), respectively. (b) Temperature dependence of the threshold field across the Al_2O_3 layer. The solid line is the best fit of the data to Eq. (4).

($J_{\mathrm{sw}}=4\mathrm{V}/R_l\mathrm{A}$, A is the electrode area), as a function of E_{th} when the V_{a} was properly adjusted. E_{th} was taken from the slope of Fig. 2(a). The J_{sw}-E_{th} variation was well fitted (solid line) with the Schottky emission described by the reported equation.[16]

$$J_{\mathrm{sw}} \propto T^2 \exp\left(\frac{-\phi_0+\beta_s E_{\mathrm{th}}^{1/2}}{k_{\mathrm{B}}T}\right), \tag{3}$$

where ϕ_0 is the Schottky barrier height (SBH) at the Pt/Al_2O_3 interface, $\beta_s=(\frac{q}{4\pi\varepsilon_0\varepsilon_{\mathrm{Al}}})$, q is the unit charge of an electron, and ε_0 is the vacuum permittivity. An $\varepsilon_{\mathrm{Al}}$ of 3.7 ± 0.4 was obtained from a fit of the data in Fig. 4(a) to Eq. (3). Hence, the refractive index (n_{Al}) was 1.9 ± 0.2, which is in good agreement with the n_{Al} of 1.7 obtained from optical measurements.[17,18] This suggests that carrier injection at the Pt/Al_2O_3 junction occurs through Schottky emission. ϕ_0 can be estimated from the temperature dependence of the E_{th} shown in Fig. 2(b). Figure 4(b) shows the change in E_{th} as a function of T. Since $J_{\mathrm{sw}}(E_{\mathrm{th}},T)=J_{\mathrm{sw}}(E_{\mathrm{th}}^0,T_0)$, where $E_{\mathrm{th}}^0=14.0$ MV/cm at $T_0=290$ K, the Eq. (4) can be obtained from Eq. (3) as follows:

$$E_{\mathrm{th}}^{1/2}(T)=\frac{2k_{\mathrm{B}}T_0}{\beta_s}\left(\frac{T}{T_0}\right)\ln\left(\frac{T_0}{T}\right)+\frac{\phi_0}{\beta_s}\left(1-\frac{T}{T_0}\right)+\left(\frac{T}{T_0}\right)(E_{\mathrm{th}}^0)^{1/2}. \tag{4}$$

The best fit of the solid line in Fig. 4(b) to Eq. (4) gives $\phi_0=1.1\pm0.2$ eV. This value is far lower than the expected SBH from the work function of Pt and the electron affinity of amorphous Al_2O_3, even though the theoretical SBH at the Pt/amorphous Al_2O_3 junction is unclear due to the lack of precise data for amorphous Al_2O_3 films. However, the lower ϕ_0 suggests that carrier emission occurs through thermionic field emission near the location ~1.1 eV from the Fermi level of Pt. This might be related to the relatively high concentration of imperfections in amorphous Al_2O_3. The SBH and barrier thickness are too large for field emission [such as direct tunneling or Fowler-Nordheim (F-N) tunneling] to occur. This is somewhat different from that for the Pt/PZT interface, as shown below.

For the Pt/PZT interface, $d_{\mathrm{f}}=4.2$ nm and V_{c} ($=V_{\mathrm{fc}}$) at $d_{\mathrm{Al}}=0$ were used to calculate the E_{th}'. Again, the same J_{sw} when $V_l=4$ V was taken and the J_{sw} vs E_{th}' plot is also shown in Fig. 4(a) (blue closed symbol).

The data fits the F-N tunneling mechanism (solid line) well, which is given by Eq. (5) (Ref. 16)

$$J_{\mathrm{sw}} \propto E^2 \exp\left(-\frac{2}{3}\frac{\alpha^*\phi_0^{3/2}}{E}\right), \tag{5}$$

where $E=E_{\mathrm{th}}'$, $\alpha^*=\alpha(m^*/m_0)^{1/2}$, $\alpha=4\pi(2m_0q)^{1/2}/h$, m^* is the effective mass for the carrier, m_0 is the mass of the static electron, and h is the Plank's constant. The best fit of the data to Eq. (5) by the solid line in Fig. 4(a) yields $(m^*/m_0)^{1/2}\phi_0^{3/2}=1.43$. Reported m^* of ferroelectric materials has the value ranging from $0.06m_0$ (Ref. 19) to $6.0m_0$.[20] Therefore, ϕ_0 value could range from 3.24 to 0.70 eV depending on the m^*. Therefore, it is difficult to accurately define ϕ_0 from the fitting due to the large uncertainty in m^*.

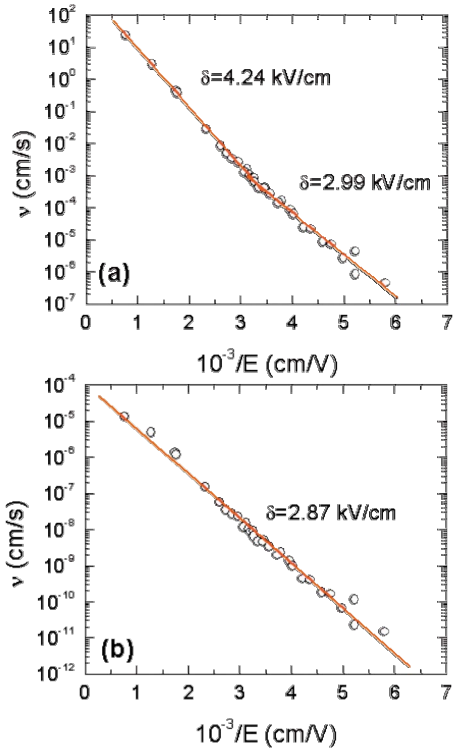

FIG. 5. (Color online) (a) The wall velocity as a function of the field reversal for single-crystal $BaTiO_3$ plotted over a broad velocity range (Fig. 6 in Ref. 23). The double lines are the lines of best fit of the data according to the Merz's law of $v \propto \exp(-\delta/E)$ at high and low-field regions with a different δ. (b) The $v/E^2 - 1/E$ semilogarithmic plot fitted linearly by a solid line according to the equation of Fowler-Nordheim tunneling with a constant δ.

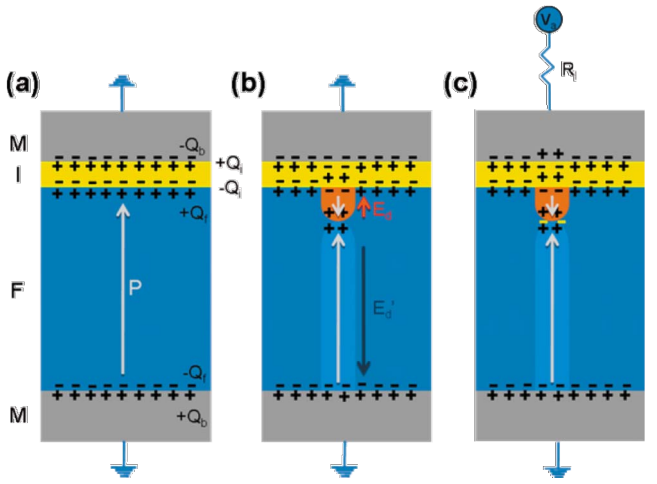

FIG. 6. (Color online) Schematic diagram showing the polarization and charge distribution (a) after the sample is prepolarized upward and the two electrodes are short circuited, (b) when a reverse domain nucleus is formed by approximately thermal fluctuation but the system is still under the short circuit condition, and (c) metal bound charge (of negative sign) is injected to the head-to-head domain boundary which is accompanied by the flow of (apparently) switching charge (of positive sign) from the voltage source to the electrode.

With work functions of 5.76 ± 0.04 eV for (111) Ir and 5.80 ± 0.06 eV for (111) Pt (Refs. 21 and 22) and an electron affinity of 3.5 ± 0.2 eV for PZT,[20] the theoretical SBH for the Pt/PZT was found to be 2.3 ± 0.2 eV for the electron if there is no contribution from the interface traps to the determination of the SBH. However, there is usually a high density of interface traps which alters the SBH. Therefore, the experimentally determined SBH from J_{sw} vs E_{th} fitting according to the F-N mechanism can be regarded as a reasonable value.

Figure 5(a) shows the results reported by Miller and Savage on the velocity of domain motion as a function of the reciprocal field (Fig. 6 in Ref. 23) in single-crystal $BaTiO_3$. According to Merz's law, v should have been proportional to $\exp(-\delta/E)$.[9] However, this can barely be true if the domain velocity changes over eight decades, as shown by the doubled-line fitting of the data in Fig. 5(a). This suggests that δ is not a constant. In comparison, v is proportional to $E^2 \exp(-\delta/E)$ using the equation developed in this study from Fowler-Nordheim tunneling. This removes the previous problem of Merz's law, as shown in Fig. 5(b), where δ is a constant. Using Eq. (5), where $v \propto E^2 \exp(-\delta/E)$, the data can be fitted perfectly with a single constant, $\delta = \frac{2}{3}\alpha^* \phi_0^{3/2}$ even for a $BaTiO_3$ single crystal. Nevertheless, it should be noted that the electrical field used for this modified model is the field over the reversed nuclei with the critical dimension.

The Landauer's paradox can be resolved by considering two facts. First, the driving force (electric field) that initiates the critical nucleus is actually quite large because the V_{fc} was applied over a few nm of the critical nuclei. Second, the extremely high W_d in the reversed regions of the nuclei can be compensated for by the by-electrode charge injection. At the initial stages of domain motion, the area for the critical nucleus is small, and W_s can be neglected compared with W_d.[7] When V_a was smaller (or R_l was larger), J_{sw} becomes smaller so that a longer time will be needed to accumulate sufficient compensation charges around the critical nucleus. Therefore, the domain motion is current limited in nature and the domain speed can be described by either Eqs. (3) or (5). In this sense, there is no well-defined down bound of V_{fc} in ferroelectrics, which is in agreement with previous studies.[6,23] Once the nucleus reaches a critical size, it grows in a stringlike path through the region where the external field is quite small.[13]

Finally, the physical (qualitative) mechanism for the charge-injection controlled polarization switching that was assumed in this study is explained in detail using the schematic diagram shown in Fig. 6. This also provides the physical reasons for maintaining a constant voltage over the ferroelectric layer during the ferroelectric switching and the application of the V_{fc} over only the reverse domain nuclei. Figure 6(a) shows the charge distributions when the metal-insulator-ferroelectric-metal (MIFM) structure is under the short circuit condition after the sample was prepolarized upward. Here, the positive ferroelectric crystal charge $(+Q_f)$ is (partly) compensated by the negative insulator charge $(-Q_i)$

at the insulator/ferroelectric (I/F) interface. It is obvious that the positive insulator charge ($+Q_i$) is compensated for by the negative metal bound charge ($-Q_b$) at the M (top electrode, TE)/I interface. At the F/bottom electrode (BE) interface the $-Q_f$ is compensated for by the positive metal bound charge ($+Q_b$). The charge compensation should not be complete due to many reasons so that there must be some depolarizing field (E_d^i) which will eventually decrease the P_s. However, this E_d^i must be far less significant compared to the depolarizing field that is operating at the moment of the reverse domain formation shown in Fig. 6(b). Therefore, E_d^i is not considered in Fig. 6(a). At a certain moment, due to the thermal fluctuation of the ferroelectric lattice a small reverse domain nucleus (embryo) is formed at the I/F interface where a certain defect (or even some residual unswitched domain) may act as the nucleation site as shown in Fig. 6(b). This temporary reverse domain nucleus formation may be related to the soft-mode lattice phonon so that its temporal formation time must be $\ll$ a few ns. However, as shown in this figure, this reverse domain nucleus is very unstable because the huge accumulation of the $+Q_f$ at the head-to-head domain boundary. The uncompensated $+Q_f$ at the domain boundary would produce a huge E_d [shown in Fig. 6(b)] of which direction is from the domain boundary to the I/F interface. This E_d destabilizes the reversed domain nucleus so that the embryo will disappear very quickly. In order to avoid this situation, an applied voltage, which is now applied positively to TE, is necessary to counteract the E_d. While the disappearance of the reverse domain nucleus (embryo) is inhibited by the applied voltage, charge injection (under this circumstance, it is $-Q_b$ that has been present in the TE) occurs to the domain boundary to stabilize the reverse domain nucleus. This circumstance is shown in Fig. 6(c). When this happened, E_d almost disappears and the reverse domain nucleus becomes stabilized. As described in detail above and in Ref. 11, at the moment of domain reversal the Al_2O_3 insulator layer becomes conducting and the charge injection readily occurs. According to this model it can be understood that the voltage is necessarily applied over the nucleation layer (including the insulator to make it conducting enough, please see Ref. 11) while the charge injection occurs. The rest of the column where the original P_s remained [in lower part of Fig. 6(b)] also becomes to have a depolarizing field, E_d', before the charge injection occurs due to the uncompensated $+Q_f$. However, it is obvious that the direction of this E_d' must be same as that of the externally applied field. The E_d' actually accelerates the domain reversal of the unswitched part of the ferroelectric material column. Once the charge injection has occurred, E_d' may also be largely decreased. Therefore, it is not necessary to apply a large portion of the applied voltage to the unswitched column where the original P_s remains. In this sense, the propagation of the reverse domain (reverse domain growth) corresponds to the progressive shift in Ti/Zr ions within a unit cell in one-unit-cell-by-one-unit-cell manner which is accompanied by the progressive transport of the injected charge ($-Q_b$) across the column also in one-unit–cell-by-one-unit-cell manner. This may readily and rapidly occur compared to the nucleation so that this again does not require a large voltage and long time. Contrary to this, the charge injection across the interfacial layer (a few nm thick) +reverse domain (also a few nm thick) requires a much larger voltage and longer time. This constitutes the basic idea for the "nucleation-controlled" ferroelectric switching. It is also noted that the applied voltage to TE to switch the domain was positive but the injected charges are of negative sign. This suggests the following: the $-Q_b$ is considered to adhere to $+Q_f$. As $+Q_f$ moves away from the I/F interface to the head-to-head domain boundary by the shift in Ti^{4+} and Zr^{4+} ions, the $-Q_b$ is accordingly moved to that boundary too. As the $-Q_b$ is transported to the domain boundary, the positive voltage source supplies the TE with the positive compensating charge ($+Q_b'$) through the load resistance R_l. This newly supplied $+Q_b'$ must correspond to the $+Q_{sw}$ of this domain region. As the R_l increases, switching current decreases so that a longer time is required to provide the TE with the necessary $+Q_b'$. The overall ferroelectric switching process can be understood as the progressive increase in the reversed domain area with time. It can be imagined that the region with locally lower V_{fc} would be reversed first. Therefore, the whole switching process may be understood as the process of the transport of a certain amount of charge ($-Q_b$) across the whole film. As the $-Q_b$ move across the whole film, the counter charge $+Q_b'$ is flown into the TE. Therefore, it should be obvious that the whole MIFM sample works as a resistor during the switching and a constant voltage drop is achieved over the ferroelectric sample during the ferroelectric switching.

Similar enlargement of switching time was previously reported. Jullian *et al.* observed almost same scale of switching time (from 10^{-7} to 10^{1} s) in ceramic modified ferroelectrics by controlling the applied field from over to below of the coercive field of the samples.[24] Therefore, such a long switching time does not suggest that the single nucleation domain waits for such a long time to achieve the huge amount of switching charge. In fact, the actual reverse domain nucleation time by thermal fluctuation must be of order of ps (phonon vibration time scale). However, most of the experimental results have shown that at least a few ns is required even without any external load resistance. This must be due to the involvement of some unavoidable parasitic resistance components even for the high-speed measurement set-up.

IV. CONCLUSION

In conclusion, the critical nuclei dimension for polarization reversal of PZT thin films was determined experimentally by measuring the V_c of $Pt/Al_2O_3/PZT/Ir$ stacked ferroelectric thin-film capacitors as a function of the Al_2O_3 layer thickness with various serially connected load resistors using the pulse-switching and P-V measurements. The critical nuclei dimension was 4.2–4.8 nm, which is in very good agreement with recent molecular-dynamics simulations.[7] To the authors' knowledge, no experimental verification of the critical dimension for the ferroelectric switching has been reported. Ferroelectric switching is a current limited process, where charge compensation through by-electrode charge injection largely mitigates the depolarization energy of the critical nuclei. Thermionic field emission for the Pt/Al_2O_3

interface and F-N tunneling for the Pt/PZT interface were also confirmed experimentally, which further strengthens the suggested switching mechanism. The classical Merz's exponential law for the domain speed in most ferroelectrics can be modified properly using the F-N tunneling mechanism. With the model suggested in this article, the behavior of the ferroelectric capacitor acting as a resistor not a capacitor during polarization switching can also be understood. With this model, the classical Landauer's paradox was also resolved. A qualitative physical model for the domain nucleation and voltage distribution during the ferroelectric switching based on the charge injection is also proposed.

ACKNOWLEDGMENT

This study was supported by the National program for 0.1 terabit NVM devices of the Korean government, and World Class University program through the Korea Science and Engineering Foundation funded by the Ministry of Education, Science and Technology (under Contract No. R31-2008-000-10075-0). The work was also supported financially by National Natural Science Foundation of China (under Contract No. 60776054), Shanghai Key Program (under Contract No. 08JC1402100), and the Program for Professor of Special Appointment (Eastern Scholar) at Shanghai Institutions of Higher Learning.

*aqjiang@fudan.edu.cn

†Corresponding author; cheolsh@snu.ac.kr

[1] R. Ahluwalia and W. Cao, Phys. Rev. B **63**, 012103 (2000).

[2] R. Ahluwalia and W. Cao, J. Appl. Phys. **93**, 537 (2003).

[3] F. Jona and G. Shirane, *Ferroelectrics Crystals* (Pergamon, Oxford, 1962).

[4] M. E. Lines and A. M. Glass, *Principles and Application of Ferroelectrics and Related Materials* (Clarendon, Oxford, 1977).

[5] R. Landauer, J. Appl. Phys. **28**, 227 (1957).

[6] R. C. Miller and G. Weinreich, Phys. Rev. **117**, 1460 (1960).

[7] Y. H. Shin, I. Grinberg, I. W. Chen, and A. M. Rappe, Nature (London) **449**, 881 (2007).

[8] S. Jesse, B. J. Rodriguez, S. Choudhury, A. P. Baddorf, I. Vrejoiu, D. Hesse, M. Alexe, E. A. Eliseev, A. N. Morozovska, J. Zhang, L.-Q. Chen, and S. V. Kalinin, Nature Mater. **7**, 209 (2008).

[9] J. W. Merz, Phys. Rev. **95**, 690 (1954).

[10] M. Molotskii, R. Kris, and G. Rosenman, J. Appl. Phys. **88**, 5318 (2000).

[11] A. Q. Jiang, H. J. Lee, G. H. Kim, and C. S. Hwang, Adv. Mater. **21**, 2870 (2009).

[12] M. Molotskii, A. Agronin, P. Urenski, M. Shvebelman, G. Rosenman, and Y. Rosenwaks, Phys. Rev. Lett. **90**, 107601 (2003).

[13] A. Q. Jiang, Y. Y. Lin, and T. A. Tang, J. Appl. Phys. **101**, 104105 (2007).

[14] D. S. Jeong, H. B. Park, and C. S. Hwang, Appl. Phys. Lett. **86**, 072903 (2005).

[15] D. S. Jeong and C. S. Hwang, Phys. Rev. B **71**, 165327 (2005).

[16] S. M. Sze, *Physics of Semiconductor Devices* (Wiley, New York, 1981).

[17] S. S. Kim, N. T. Gabriel, W. B. Song, and J. J. Talghader, Opt. Express **15**, 16285 (2007).

[18] D. Riihela, M. Ritala, R. Matero, and M. Leskela, Thin Solid Films **289**, 250 (1996).

[19] J. C. Shin, J. Park, C. S. Hwang, and H. J. Kim, J. Appl. Phys. **86**, 506 (1999).

[20] J. F. Scott, *Ferroelectric Memories* (Springer, Berlin, 2000).

[21] H. Kawano, Appl. Surf. Sci. **254**, 7187 (2008).

[22] H. Sa'adi and B. Hamad, J. Phys. Chem. Solids **69**, 2457 (2008).

[23] R. C. Miller and A. Savage, Phys. Rev. **115**, 1176 (1959).

[24] C. Jullian, J. F. Li, and D. Viehland, Appl. Phys. Lett. **83**, 1196 (2003).